

# Electronic structure of $(\text{Ga}_{55}\text{In}_{45})_2\text{S}_{300}$ and $(\text{Ga}_{54.59}\text{In}_{44.66}\text{Er}_{0.75})_2\text{S}_{300}$ single crystals

O. Y. Khyzhun<sup>1</sup> · V. V. Halyan<sup>2</sup> · I. V. Danyliuk<sup>3</sup> · I. A. Ivashchenko<sup>3</sup>

Received: 7 October 2015 / Accepted: 26 November 2015 / Published online: 9 December 2015  
© Springer Science+Business Media New York 2015

**Abstract** We report on studies of the X-ray photoelectron core-level and valence-band spectra for pristine and  $\text{Ar}^+$ -ion bombarded surfaces of  $(\text{Ga}_{55}\text{In}_{45})_2\text{S}_{300}$  and  $(\text{Ga}_{54.59}\text{In}_{44.66}\text{Er}_{0.75})_2\text{S}_{300}$  single crystals grown by solution-melt technique. The  $(\text{Ga}_{55}\text{In}_{45})_2\text{S}_{300}$  and  $(\text{Ga}_{54.59}\text{In}_{44.66}\text{Er}_{0.75})_2\text{S}_{300}$  single crystals were found to be very rigid with respect to  $\text{Ar}^+$ -ion bombardment. In particular, such a treatment did not cause any significant changes of values of the binding energies of core-level electrons as well as of the shapes of the XPS core-level and valence-band spectra of  $(\text{Ga}_{55}\text{In}_{45})_2\text{S}_{300}$  and  $(\text{Ga}_{54.59}\text{In}_{44.66}\text{Er}_{0.75})_2\text{S}_{300}$  single crystal surfaces. We measured for the  $(\text{Ga}_{55}\text{In}_{45})_2\text{S}_{300}$  compound the X-ray emission bands representing the energy distribution of mainly the valence  $\text{S}p$  and  $\text{Ga}p$  states and compared them on a common energy scale with the XPS valence-band spectrum. The comparison allows us for concluding that the  $\text{S}3p$  and  $\text{Ga}4p$  states contribute mainly at the top and in the central portion of the valence band of  $(\text{Ga}_{55}\text{In}_{45})_2\text{S}_{300}$ , respectively. In addition, we have also detected at ambient conditions a strong photoluminescence of the  $(\text{Ga}_{54.59}\text{In}_{44.66}\text{Er}_{0.75})_2\text{S}_{300}$  single crystal with a maximum at 810 nm for the excitation wavelength of 532 nm. Our results indicate that the  $(\text{Ga}_{54.59}\text{In}_{44.66}\text{Er}_{0.75})_2\text{S}_{300}$  single crystal is a very

promising material for its application in optoelectronic technologies.

## 1 Introduction

A variety of ternary layered semiconducting chalcogenides forming in the quasibinary  $\text{Ga}_2\text{S}(\text{Se})_3\text{--In}_2\text{S}(\text{Se})_3$  systems have attracted in recent years significant attention from both a scientific and technological viewpoint because of their rather useful physical properties which make these compounds to be considered very promising materials for application in solar energy devices [1–4]. For example, at least six ternary compounds with a common formula  $\text{Ga}_x\text{In}_{2-x}\text{S}_3$  have been established to exist in the quasibinary  $\text{Ga}_2\text{S}_3\text{--In}_2\text{S}_3$  system, namely  $\text{Ga}_2\text{In}_8\text{S}_{15}$  (or  $\text{Ga}_{0.4}\text{In}_{1.6}\text{S}_3$ ),  $\text{Ga}_{0.5}\text{In}_{1.5}\text{S}_3$ ,  $\text{Ga}_2\text{In}_4\text{S}_9$  (or  $\text{Ga}_{0.67}\text{In}_{1.33}\text{S}_3$ ),  $\text{GaInS}_3$ ,  $(\text{Ga}_{55}\text{In}_{45})_2\text{S}_{300}$  (or  $\text{Ga}_{1.1}\text{In}_{0.9}\text{S}_3$ ) and  $\text{Ga}_6\text{In}_4\text{S}_{15}$  (or  $\text{Ga}_{1.2}\text{In}_{0.8}\text{S}_3$ ) [5–14]. In particular, the ternary sulphide  $(\text{Ga}_{55}\text{In}_{45})_2\text{S}_{300}$ , which was synthesized for the first time very recently in Ref. [14], was found to be doped rather easily with  $\text{Er}^{3+}$  ions. The formation of the  $(\text{Ga}_{54.59}\text{In}_{44.66}\text{Er}_{0.75})_2\text{S}_{300}$  compound leads to increasing the absorption coefficient in the 520–1600 nm spectral range as compared with its parent compound, namely  $(\text{Ga}_{55}\text{In}_{45})_2\text{S}_{300}$ , and to the appearance of five additional absorption bands on the optical absorption spectrum. These bands have been detected at about 530, 660, 810, 980 and 1530 nm in the visible and near-infrared range of the optical absorption spectrum of  $(\text{Ga}_{54.59}\text{In}_{44.66}\text{Er}_{0.75})_2\text{S}_{300}$ . The bands have been established to be caused by intra-center transitions from the ground state  $^4\text{I}_{15/2}$  to the excited levels  $^2\text{H}_{11/2}$ ,  $^4\text{F}_{9/2}$ ,  $^4\text{I}_{9/2}$ ,  $^4\text{I}_{11/2}$  and  $^4\text{I}_{13/2}$  associated with  $\text{Er}^{3+}$  ions [14]. Additionally, the excitation of the photoluminescence spectra by using an LDM532U laser of 150 mW at 532 and 980 nm radiation

✉ O. Y. Khyzhun  
khyzhun@ukr.net; khyzhun@ipms.kiev.ua

<sup>1</sup> Institute for Problems of Materials Science, National Academy of Sciences of Ukraine, 3 Krzhyzhanivsky Street, Kiev 03142, Ukraine

<sup>2</sup> Department of General Physics, Eastern European National University, 13 Voli Avenue, Lutsk 43025, Ukraine

<sup>3</sup> Department of Inorganic and Physical Chemistry, Eastern European National University, 13 Voli Avenue, Lutsk 43025, Ukraine

maxima has revealed in the  $(\text{Ga}_{54.59}\text{In}_{44.66}\text{Er}_{0.75})_2\text{S}_{300}$  compound a strong luminescence in the spectral range of 1450–1650 nm. Furthermore, it has been found that the intensity and the effective width of photoluminescence of  $(\text{Ga}_{54.59}\text{In}_{44.66}\text{Er}_{0.75})_2\text{S}_{300}$  single crystal depends significantly on the excitation wavelength and the exchange of energy between the host and  $\text{Er}^{3+}$  ions in this compound [14].

To the best of our knowledge, electronic structure of the  $(\text{Ga}_{55}\text{In}_{45})_2\text{S}_{300}$  (or  $\text{Ga}_{1.1}\text{In}_{0.9}\text{S}_3$ ) compound has not been studied yet. Therefore, in the present work we use the possibilities of the X-ray photoelectron spectroscopy (XPS) method to evaluate the binding energies of core-level electrons of atoms constituting the  $(\text{Ga}_{55}\text{In}_{45})_2\text{S}_{300}$  compound as well to measure its XPS valence-band spectrum. To gain our goal, we use the high-quality  $(\text{Ga}_{55}\text{In}_{45})_2\text{S}_{300}$  single crystal grown recently by solution-melt technique [14]. A number of experimental studies and first-principles band-structure calculations of ternary and quaternary gallium-containing sulfides (selenides) reveal that their electronic structure is characterized by significant contributions of the valence S(Se)  $p$  and Ga  $p$  states in the valence band region (see, e.g., Refs. [15–21]). Therefore, in the present work we also use the X-ray emission spectroscopy (XES) method to measure for the  $(\text{Ga}_{55}\text{In}_{45})_2\text{S}_{300}$  single crystal the XES S  $K\beta_{1,3}$  and Ga  $K\beta_2$  bands representing the energy distribution of mainly the S  $3p$  and Ga  $4p$  states, respectively, and to compare them on a common energy scale with the XPS valence-band spectrum of the compound under consideration. It is known that the chemical state/composition of the top surface layer with thickness of about 30–50 Å is well probed using XPS spectra excited either with Mg  $K\alpha$  or Al  $K\alpha$  sources [22]. Thus, the influence of middle-energy  $\text{Ar}^+$ -ion bombardment on the valence-band and constituent element core-level XPS spectra of  $(\text{Ga}_{55}\text{In}_{45})_2\text{S}_{300}$  single-crystal surface is also studied in the present study because this method of surface cleaning is widely applied in epitaxial technologies. In order to explore the influence of doping by  $\text{Er}^{3+}$  ions on the electronic structure of  $(\text{Ga}_{55}\text{In}_{45})_2\text{S}_{300}$ , the XPS core-level and valence-band spectra of the  $(\text{Ga}_{54.59}\text{In}_{44.66}\text{Er}_{0.75})_2\text{S}_{300}$  single crystal surface, both pristine and  $\text{Ar}^+$  ion-bombarded, are investigated in the present work as well. In addition, we report also on measurements at room temperature of the photoluminescence spectrum for the  $(\text{Ga}_{54.59}\text{In}_{44.66}\text{Er}_{0.75})_2\text{S}_{300}$  single crystal in the range of 600–1000 nm.

## 2 Experimental

For the present experimental studies we used the  $(\text{Ga}_{55}\text{In}_{45})_2\text{S}_{300}$  and  $(\text{Ga}_{54.59}\text{In}_{44.66}\text{Er}_{0.75})_2\text{S}_{300}$  single crystals grown very recently by solution-melt method as described in detail in Ref. [14]. Briefly, the crystal growth of the

starting alloys was performed at maximum temperature 1200 K in evacuated quartz containers placed in two-zone furnaces. The temperature gradient at the solid-melt interface was set to be 20 K/cm during the synthesis. After melting the batches, the containers were lowered at a rate of 5 mm/day, followed by annealing with 100 h duration and after that the lowering rate was set to be again 5 mm/day. The synthesis process was continued by cooling the furnaces to 820 K at a rate of 50–70 K/day followed by switching off the furnaces. The orange-yellow crystals (diameter  $\sim$  14 mm, length  $\sim$  20 mm) were grown. As an example, Fig. 1 presents a photo of pieces of the  $(\text{Ga}_{55}\text{In}_{45})_2\text{S}_{300}$  and  $(\text{Ga}_{54.59}\text{In}_{44.66}\text{Er}_{0.75})_2\text{S}_{300}$  single crystals used in the present experiments. Further, for the present XPS and XES measurements the crystals under consideration were prepared in shapes of thin plates with the following dimensions: length  $\sim$  7–8 mm, width  $\sim$  6.5 mm, and height  $\sim$  1.5 mm. The plates were polished following the technique reported in detail in Ref. [23] to gain their high-quality optical surfaces. Measurements of XPS valence-band and core-level spectra of the  $(\text{Ga}_{55}\text{In}_{45})_2\text{S}_{300}$  and  $(\text{Ga}_{54.59}\text{In}_{44.66}\text{Er}_{0.75})_2\text{S}_{300}$  single crystals were performed in an ion-pumped chamber having a base pressure less than  $5 \times 10^{-10}$  mbar of the UHV-Analysis-System assembled by SPECS Surface Nano Analysis Company (Berlin, Germany). The UHV-Analysis-System system is equipped with a PHOIBOS 150 hemispherical analyzer. The XPS spectra were excited by an Al  $K\alpha$  source of X-ray radiation ( $E = 1486.6$  eV) and were collected at constant pass energy of 30 eV. The energy scale of the XPS spectrometer was calibrated by setting the measured Au  $4f_{7/2}$  and Cu  $2p_{3/2}$  binding energies of pure reference metals to  $84.00 \pm 0.05$  and  $932.66 \pm 0.05$  eV, respectively, with respect to the Fermi energy,  $E_F$ . The charging effects were

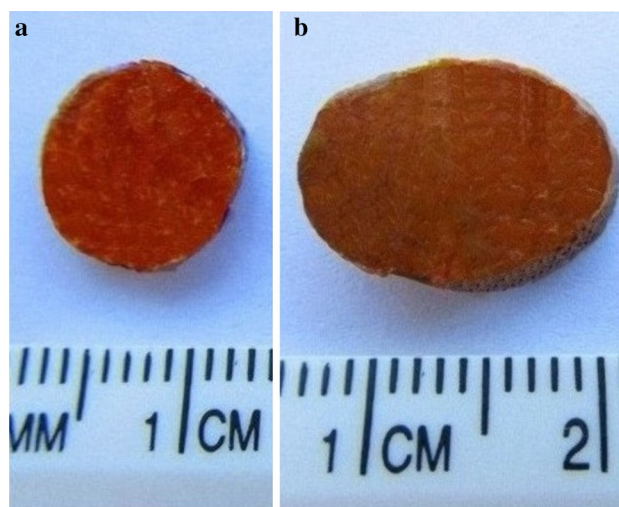


**Fig. 1** Photos of the single crystals used in the present experiments: **a**  $(\text{Ga}_{55}\text{In}_{45})_2\text{S}_{300}$  and **b**  $(\text{Ga}_{54.59}\text{In}_{44.66}\text{Er}_{0.75})_2\text{S}_{300}$

taken into account in reference to the C 1s line (284.6 eV) of adventitious carbon as suggested for gallium- and/or indium-bearing chalcogenides [18, 20, 24]. In order to remove surface contaminations, irradiation of crystal surfaces has been made by Ar<sup>+</sup> ions with energy of 3.0 keV over 5 min at an ion current density of 14 μA/cm<sup>2</sup>. A total Ar<sup>+</sup> flux was estimated to be  $\sim 5.3 \times 10^{16}$  ions/cm<sup>2</sup>. The method of the above surface treatment is completely the same as we used earlier for a series of gallium- and/or indium-bearing chalcogenides [18, 24]. The fluorescent X-ray emission S Kβ<sub>1,3</sub> (K → M<sub>II,III</sub> transition) and Ga Kβ<sub>2</sub> (K → N<sub>II,III</sub> transition) bands representing the energy distribution of the valence S *p* and Ga *p* states, respectively, were measured by using a Johann-type DRS-2M spectrograph equipped with an X-ray BHV-7 tube (gold anode) adopting the technique described in detail in Ref. [25]. As disperse elements, quartz crystals with the (10 $\bar{1}$ 0) and (0001) reflecting planes were used when recording the XES S Kβ<sub>1,3</sub> and Ga Kβ<sub>2</sub> bands, respectively. The spectrograph energy resolutions were estimated to be about 0.3 eV in the energy regions corresponding to the positions of the measuring XES bands.

The photoluminescence spectrum of the (Ga<sub>54.59</sub>In<sub>44.66</sub>Er<sub>0.75</sub>)<sub>2</sub>S<sub>300</sub> single crystal was explored at 300 K employing an LDM5324 laser of 150 mW power with 532 nm radiation maximum. The photoluminescence intensity was measured by using an MDR-206 monochromator equipped with a Si-based photodetector. The spectrum was recorded in the range of 600–1000 nm.

### 3 Results and discussion

Figure 2 presents the survey XPS spectra of pristine and Ar<sup>+</sup>-ion bombarded surfaces of the (Ga<sub>55</sub>In<sub>45</sub>)<sub>2</sub>S<sub>300</sub> and (Ga<sub>54.59</sub>In<sub>44.66</sub>Er<sub>0.75</sub>)<sub>2</sub>S<sub>300</sub> single crystals. From the figure, one can see that all the spectral features, except the C(O) 1s levels and the O KLL Auger line, are attributed to constituent element core-levels or Auger lines. XPS data presented in Fig. 2 reveal that no active chemical interaction with oxygen occurs when the (Ga<sub>55</sub>In<sub>45</sub>)<sub>2</sub>S<sub>300</sub> and (Ga<sub>54.59</sub>In<sub>44.66</sub>Er<sub>0.75</sub>)<sub>2</sub>S<sub>300</sub> single crystal surfaces contact with air for a comparatively long time (a couple of weeks). From the survey XPS spectra presented in Fig. 2, it is apparent that relative intensities of the O 1s lines are rather low on the pristine surfaces of the (Ga<sub>55</sub>In<sub>45</sub>)<sub>2</sub>S<sub>300</sub> and (Ga<sub>54.59</sub>In<sub>44.66</sub>Er<sub>0.75</sub>)<sub>2</sub>S<sub>300</sub> single crystals. Furthermore, we have detected no traces of oxygen presence as a result of the Ar<sup>+</sup>-ion bombardment of the (Ga<sub>55</sub>In<sub>45</sub>)<sub>2</sub>S<sub>300</sub> and (Ga<sub>54.59</sub>In<sub>44.66</sub>Er<sub>0.75</sub>)<sub>2</sub>S<sub>300</sub> single crystal surfaces. Therefore, the present XPS results reveal low hygroscopicity of the (Ga<sub>55</sub>In<sub>45</sub>)<sub>2</sub>S<sub>300</sub> and (Ga<sub>54.59</sub>In<sub>44.66</sub>Er<sub>0.75</sub>)<sub>2</sub>S<sub>300</sub> single crystal surfaces. This property is extremely important for

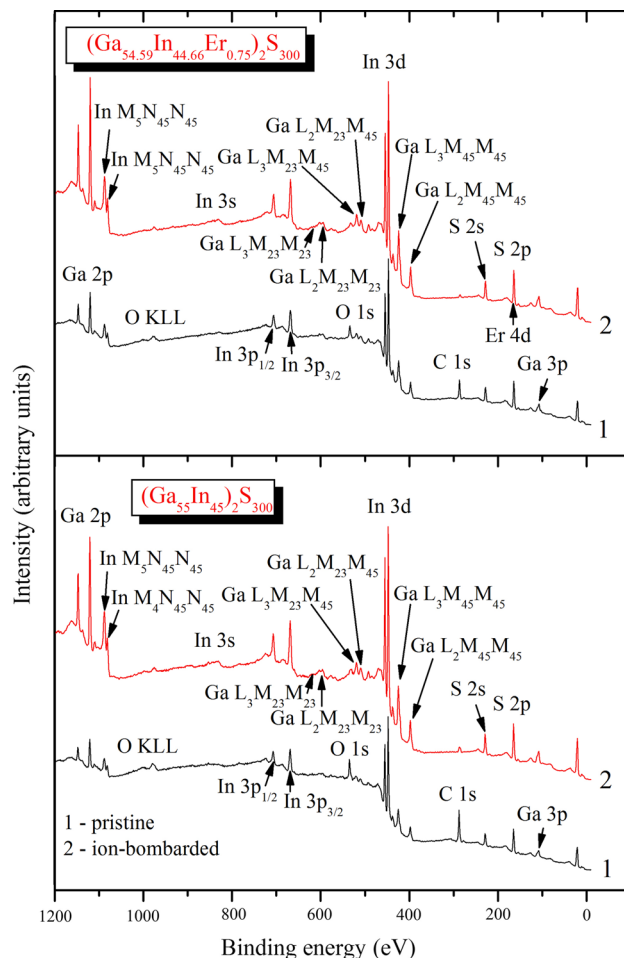


**Fig. 2** Survey XPS spectra recorded for (1) pristine and (2) Ar<sup>+</sup> ion-bombarded surface of the (Ga<sub>55</sub>In<sub>45</sub>)<sub>2</sub>S<sub>300</sub> and (Ga<sub>54.59</sub>In<sub>44.66</sub>Er<sub>0.75</sub>)<sub>2</sub>S<sub>300</sub> single crystals

handling these materials in optoelectronic devices operating at ambient conditions. It is worth also mentioning that, the shapes of the C 1s core-level lines (not presented here) for the pristine (Ga<sub>55</sub>In<sub>45</sub>)<sub>2</sub>S<sub>300</sub> and (Ga<sub>54.59</sub>In<sub>44.66</sub>Er<sub>0.75</sub>)<sub>2</sub>S<sub>300</sub> single crystal surfaces were established to be narrow, with their maxima fixed at 284.6 eV and without any features on their higher binding energy slopes that can be related to carbonate formation. This fact allows for concluding that the C 1s core-level spectra recorded for the pristine surfaces of the (Ga<sub>55</sub>In<sub>45</sub>)<sub>2</sub>S<sub>300</sub> and (Ga<sub>54.59</sub>In<sub>44.66</sub>Er<sub>0.75</sub>)<sub>2</sub>S<sub>300</sub> single crystals are related exclusively to hydrocarbons adsorbed from laboratory air. It is necessary also to indicate that because of the small content of Er atoms in the (Ga<sub>54.59</sub>In<sub>44.66</sub>Er<sub>0.75</sub>)<sub>2</sub>S<sub>300</sub> single crystal and due to the fact that the most intensive XPS core-level line associated with erbium when exciting with an Al Kα source of X-ray radiation, namely the Er 4d line, superimposes the S 2p line, we could not resolve the XPS Er 4d spectrum in our experiments carried out for the (Ga<sub>54.59</sub>In<sub>44.66</sub>Er<sub>0.75</sub>)<sub>2</sub>S<sub>300</sub> sample.

**Table 1** Binding energies (in eV<sup>a</sup>) of constituent element core levels of pristine and Ar<sup>+</sup>-ion bombarded surfaces of the (Ga<sub>55</sub>In<sub>45</sub>)<sub>2</sub>S<sub>300</sub> and (Ga<sub>54.59</sub>In<sub>44.66</sub>Er<sub>0.75</sub>)<sub>2</sub>S<sub>300</sub> single crystals

Core-level	(Ga <sub>55</sub> In <sub>45</sub> ) <sub>2</sub> S <sub>300</sub> /pristine surface	(Ga <sub>55</sub> In <sub>45</sub> ) <sub>2</sub> S <sub>300</sub> /Ar <sup>+</sup> -ion bombarded surface	(Ga <sub>54.59</sub> In <sub>44.66</sub> Er <sub>0.75</sub> ) <sub>2</sub> S <sub>300</sub> /pristine surface	(Ga <sub>54.59</sub> In <sub>44.66</sub> Er <sub>0.75</sub> ) <sub>2</sub> S <sub>300</sub> /Ar <sup>+</sup> -ion bombarded surface
S 2p	161.65	161.61	161.70	161.73
In 3d <sub>5/2</sub>	444.57	444.48	444.53	444.61
In 3d <sub>3/2</sub>	452.16	452.07	452.11	452.19
Ga 2p <sub>3/2</sub>	1117.63	1117.48	1117.55	1117.66
Ga 2p <sub>1/2</sub>	1144.51	1144.43	1144.56	1144.61

<sup>a</sup> Uncertainty of the measurements is ±0.05 eV

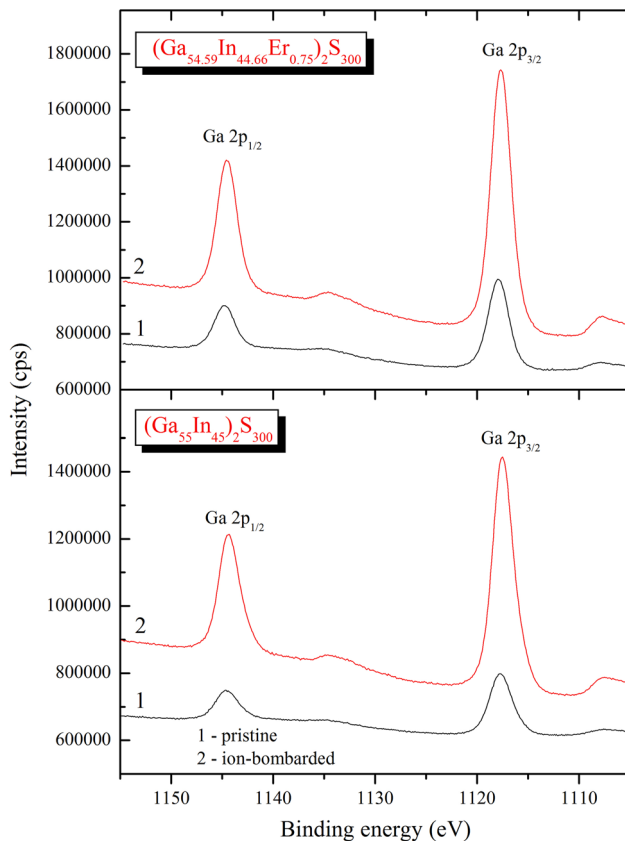


**Fig. 3** Detailed XPS Ga 2p core-level spectra recorded for (1) pristine and (2) Ar<sup>+</sup> ion-bombarded surfaces of the (Ga<sub>55</sub>In<sub>45</sub>)<sub>2</sub>S<sub>300</sub> and (Ga<sub>54.59</sub>In<sub>44.66</sub>Er<sub>0.75</sub>)<sub>2</sub>S<sub>300</sub> single crystals

Values of binding energies of the most important core-level electrons of the (Ga<sub>55</sub>In<sub>45</sub>)<sub>2</sub>S<sub>300</sub> and (Ga<sub>54.59</sub>In<sub>44.66</sub>Er<sub>0.75</sub>)<sub>2</sub>S<sub>300</sub> single crystals that were measured for both pristine and Ar<sup>+</sup>-ion bombarded surfaces, are listed in Table 1. In addition, the main XPS core-level spectra associated with Ga, In, and S atoms recorded in our experiments for the (Ga<sub>55</sub>In<sub>45</sub>)<sub>2</sub>S<sub>300</sub> and (Ga<sub>54.59</sub>In<sub>44.66</sub>Er<sub>0.75</sub>)<sub>2</sub>S<sub>300</sub> single crystal surfaces before and after their Ar<sup>+</sup>-ion bombardment are presented in Figs. 3, 4 and 5. Our XPS results reveal significant rigidity of the (Ga<sub>55</sub>In<sub>45</sub>)<sub>2</sub>S<sub>300</sub> and (Ga<sub>54.59</sub>In<sub>44.66</sub>Er<sub>0.75</sub>)<sub>2</sub>S<sub>300</sub> single crystal

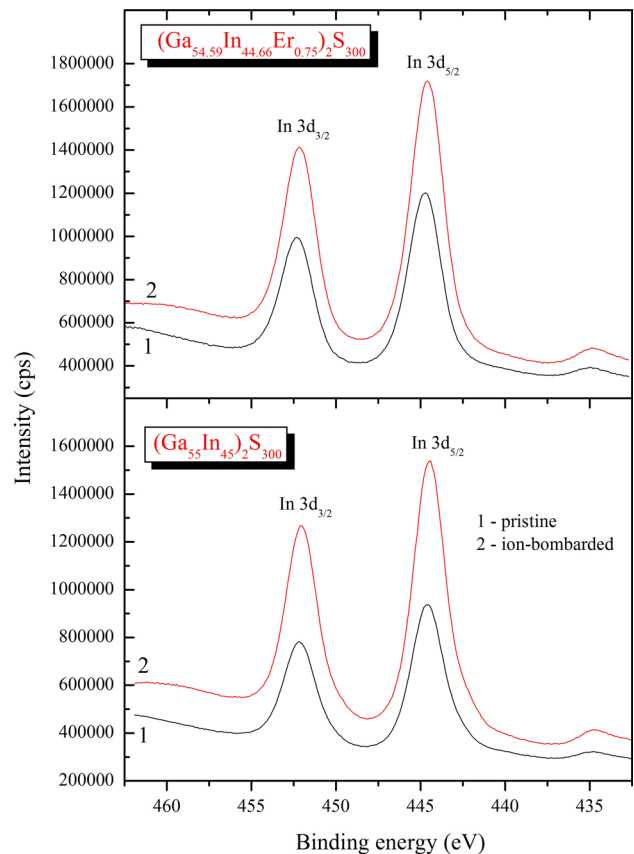


**Fig. 4** Detailed XPS In 3d core-level spectra recorded for (1) pristine and (2) Ar<sup>+</sup> ion-bombarded surfaces of the (Ga<sub>55</sub>In<sub>45</sub>)<sub>2</sub>S<sub>300</sub> and (Ga<sub>54.59</sub>In<sub>44.66</sub>Er<sub>0.75</sub>)<sub>2</sub>S<sub>300</sub> single crystals

surfaces with respect to the Ar<sup>+</sup>-ion bombardment. As can be seen from Figs. 3, 4 and 5, Ar<sup>+</sup>-ion bombardment of the (Ga<sub>55</sub>In<sub>45</sub>)<sub>2</sub>S<sub>300</sub> and (Ga<sub>54.59</sub>In<sub>44.66</sub>Er<sub>0.75</sub>)<sub>2</sub>S<sub>300</sub> single crystal surfaces with 3.0 keV Ar<sup>+</sup> ions during 5 min induced no significant changes of binding energy values of constituent element core-level electrons (Table 1) or shapes of the XPS core-level spectra. Furthermore, the present XPS results reveal the Ar<sup>+</sup>-ion bombardment at the fluence of 5.3 × 10<sup>16</sup> ions/cm<sup>2</sup> did not alter the chemical stoichiometry and concentration of individual elements of the (Ga<sub>55</sub>In<sub>45</sub>)<sub>2</sub>S<sub>300</sub> and (Ga<sub>54.59</sub>In<sub>44.66</sub>Er<sub>0.75</sub>)<sub>2</sub>S<sub>300</sub> single



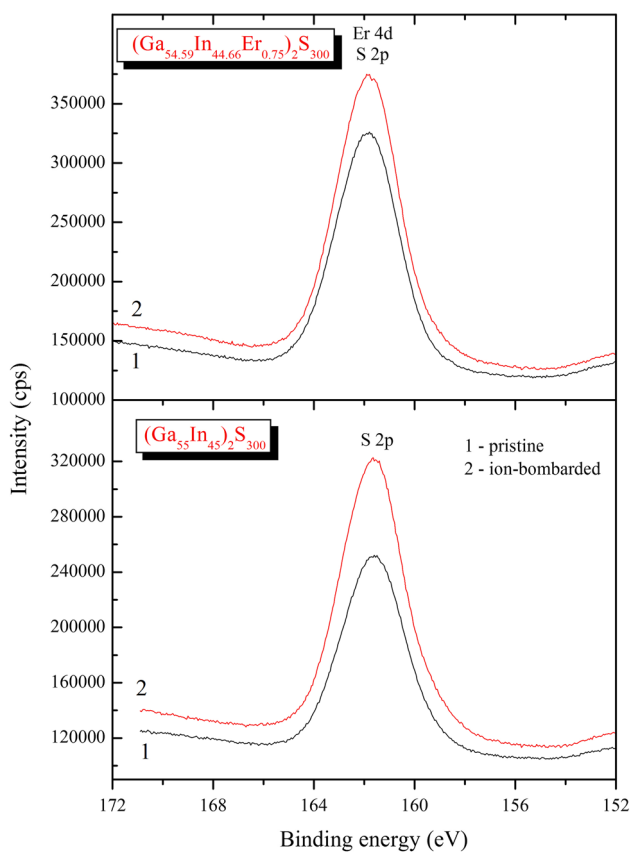


**Fig. 5** Detailed XPS  $S\ 2p$  core-level spectra recorded for (1) pristine and (2)  $\text{Ar}^+$  ion-bombarded surfaces of the  $(\text{Ga}_{55}\text{In}_{45})_2\text{S}_{300}$  and  $(\text{Ga}_{54.59}\text{In}_{44.66}\text{Er}_{0.75})_2\text{S}_{300}$  single crystals

crystal surfaces. The above mentioned  $\text{Ar}^+$ -ion treatment did not cause the visible changes of the energy distribution of the electronic states within the valence band regions of the  $(\text{Ga}_{55}\text{In}_{45})_2\text{S}_{300}$  and  $(\text{Ga}_{54.59}\text{In}_{44.66}\text{Er}_{0.75})_2\text{S}_{300}$  single crystals, as Fig. 6 demonstrates.

It is necessary also to indicate that the effect of doping the  $(\text{Ga}_{55}\text{In}_{45})_2\text{S}_{300}$  compound by  $\text{Er}^{3+}$  ions leading to the formation of the  $(\text{Ga}_{54.59}\text{In}_{44.66}\text{Er}_{0.75})_2\text{S}_{300}$  sample has been detected to be rather minor on the XPS core-level and valence band spectra. As can be seen from Figs. 3, 4 and 5 and data listed in Table 1, when going from  $(\text{Ga}_{55}\text{In}_{45})_2\text{S}_{300}$  to  $(\text{Ga}_{54.59}\text{In}_{44.66}\text{Er}_{0.75})_2\text{S}_{300}$ , we did not detect neither any noticeable changes of shapes of the XPS core-level and valence-band spectra nor shifts of the binding energy position of constituent element core levels. This means that the insertion of  $\text{Er}^{3+}$  ions into the  $(\text{Ga}_{55}\text{In}_{45})_2\text{S}_{300}$  lattice resulting in the formation of the  $(\text{Ga}_{54.59}\text{In}_{44.66}\text{Er}_{0.75})_2\text{S}_{300}$  compound does not alter significantly the peculiarities of the chemical bonding of the parent compound. In the above sequence of compounds, the energy distribution of the electronic states within the valence band regions does not change within the accuracy of the present XPS measurements (see Fig. 6).

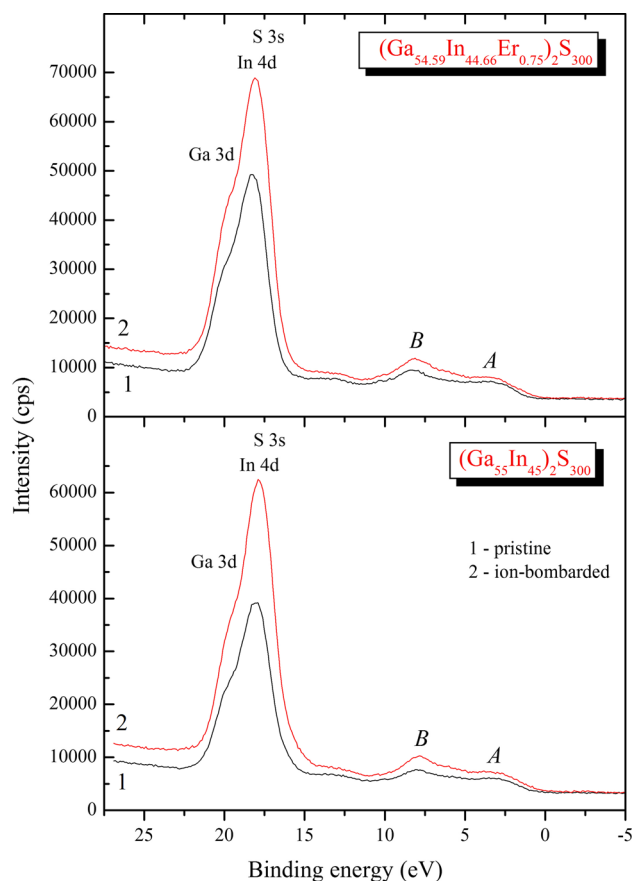


**Fig. 6** XPS valence-band spectra (including some upper core-levels) recorded for (1) pristine and (2)  $\text{Ar}^+$  ion-bombarded surfaces of the  $(\text{Ga}_{55}\text{In}_{45})_2\text{S}_{300}$  and  $(\text{Ga}_{54.59}\text{In}_{44.66}\text{Er}_{0.75})_2\text{S}_{300}$  single crystals

Figure 7 presents comparison of the X-ray emission  $\text{Ga}\ \text{K}\beta_2$  and  $\text{S}\ \text{K}\beta_{1,3}$  bands of the  $(\text{Ga}_{55}\text{In}_{45})_2\text{S}_{300}$  single crystal provided that a common energy scale is used. The technique of matching the above X-ray emission bands of  $(\text{Ga}_{55}\text{In}_{45})_2\text{S}_{300}$  on a common energy scale is analogous to that described in detail in Ref. [26] and it is commonly used in experimental X-ray spectroscopy studies of the electronic structure of solids [27–29]. The XPS valence-band spectrum of the  $(\text{Ga}_{55}\text{In}_{45})_2\text{S}_{300}$  single crystal is also plotted in Fig. 7, for comparison. It is worth indicating that the zero of energy of the X-ray emission  $\text{Ga}\ \text{K}\beta_2$  and  $\text{S}\ \text{K}\beta_{1,3}$  bands and the XPS valence-band spectrum of  $(\text{Ga}_{55}\text{In}_{45})_2\text{S}_{300}$  (Fig. 7) corresponds to the position of the Fermi level of the PHOIBOS 150 hemispherical energy analyzer. As can be seen from comparison of the XPS and XES spectra plotted in Fig. 7, energy position of the fine-structure peculiarity A of the XPS valence-band spectrum of  $(\text{Ga}_{55}\text{In}_{45})_2\text{S}_{300}$  corresponds to the position of the maximum *a* of the X-ray emission  $\text{S}\ \text{K}\beta_{1,3}$  band. The latter band consists of another fine-structure peculiarity, namely *b*, which is positioned on a common energy scale between the peculiarities A and B of the XPS valence-band spectrum

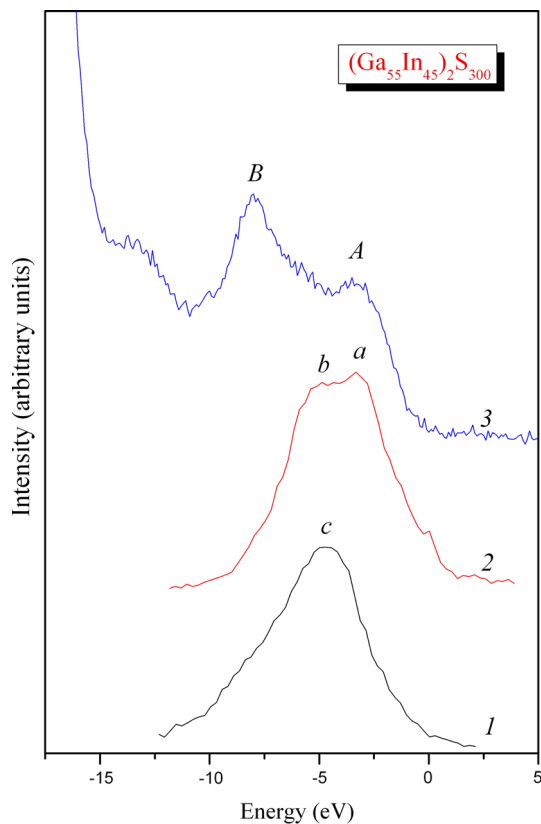


**Fig. 7** Comparison on a common energy scale of the X-ray emission (1) Ga  $K\beta_2$  and (2) S  $K\beta_{1,3}$  bands and (3) the XPS valence-band spectrum of the  $(\text{Ga}_{55}\text{In}_{45})_2\text{S}_{300}$  single crystal

of  $(\text{Ga}_{55}\text{In}_{45})_2\text{S}_{300}$ . In addition, as can be seen from Fig. 7, the main maximum *c* of the X-ray emission Ga  $K\beta_2$  band coincides with the energy position of the fine-structure peculiarity *b* of the XES S  $K\beta_{1,3}$  band of the  $(\text{Ga}_{55}\text{In}_{45})_2\text{S}_{300}$  compound. Therefore, the above experimental results reveal that the main contributions of the Ga  $4p$  states should occur in the central portion of the valence band of  $(\text{Ga}_{55}\text{In}_{45})_2\text{S}_{300}$ , while the S  $3p$  states contribute mainly at its top, with their contributions in other portions of the valence band region.

Figure 8 demonstrates the photoluminescence (PL) spectrum of the  $(\text{Ga}_{54.59}\text{In}_{44.66}\text{Er}_{0.75})_2\text{S}_{300}$  single crystal at 300 K that was explored in the range of 600–1000 nm. For the  $(\text{Ga}_{55}\text{In}_{45})_2\text{S}_{300}$  single crystal we did not detect any PL irradiation in the spectral range of 600–1650 nm. Figure 8 reveals for the  $(\text{Ga}_{54.59}\text{In}_{44.66}\text{Er}_{0.75})_2\text{S}_{300}$  single crystal the existence of a rather intensive PL band with its maximum at 810 nm. Very recently for this crystal the PL band with its maximum positioned at 1530 nm was detected in Ref. [14]. The above PL bands correspond to intra-center transitions  $^4I_{9/2} \rightarrow ^4I_{15/2}$  (in the case of the PL band centered at 810 nm) and  $^4I_{13/2} \rightarrow ^4I_{15/2}$  (for the PL band with its maximum at 1530 nm) in  $\text{Er}^{3+}$  ions. It is worth mentioning

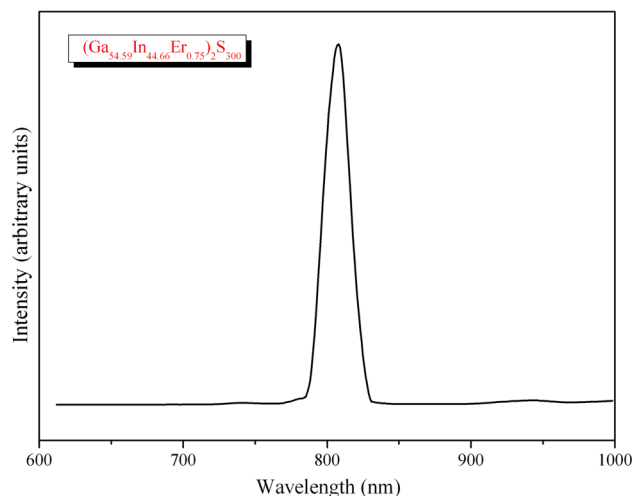


**Fig. 8** Photoluminescence spectrum of the  $(\text{Ga}_{54.59}\text{In}_{44.66}\text{Er}_{0.75})_2\text{S}_{300}$  single crystal at 300 K

that unlike the  $(\text{Ga}_{54.59}\text{In}_{44.66}\text{Er}_{0.75})_2\text{S}_{300}$  single crystal, in chalcogenide glasses the PL excitation is accompanied by a large number of emission bands [30–32]. One can assume that in the case of the amorphous glasses,  $\text{Er}^{3+}$  ions can occupy several positions that differ from it other by the nearest surroundings. Therefore, erbium ions that occupy different positions in the amorphous glasses can cause a variety of emission bands. Crystals are characterized by a high degree of ordering of atoms in lattice sites. As a result, in the case of the  $(\text{Ga}_{54.59}\text{In}_{44.66}\text{Er}_{0.75})_2\text{S}_{300}$  single crystal, doping  $\text{Er}^{3+}$  ions possess a limited number of positions in the cation sublattice that is associated with the formation of defects in the crystal [14]. Accordingly, the present PL results coupled with those reported in Ref. [14] allow for concluding that the existence of the two intensive emission bands in the near infrared spectral range is characteristic of the  $(\text{Ga}_{54.59}\text{In}_{44.66}\text{Er}_{0.75})_2\text{S}_{300}$  single crystal. This fact suggests that the  $(\text{Ga}_{54.59}\text{In}_{44.66}\text{Er}_{0.75})_2\text{S}_{300}$  single crystal is a very promising material for its application in optoelectronic technologies, in particular luminophores, wide-band optical filters, light-emitting diodes, optical amplifiers, etc.

## 4 Conclusions

Electronic structure of the  $(\text{Ga}_{55}\text{In}_{45})_2\text{S}_{300}$  and  $(\text{Ga}_{54.59}\text{In}_{44.66}\text{Er}_{0.75})_2\text{S}_{300}$  single crystals grown by solution-melt technique was explored in the present work based on X-ray spectroscopy data. In particular, both pristine and 3.0 keV  $\text{Ar}^+$ -ion bombarded surfaces of the  $(\text{Ga}_{55}\text{In}_{45})_2\text{S}_{300}$  and  $(\text{Ga}_{54.59}\text{In}_{44.66}\text{Er}_{0.75})_2\text{S}_{300}$  single crystals have been studied by XPS. It has been established that the  $\text{Ar}^+$ -ion bombardment does not induce any significant structural modifications in the top surface layers of the crystals under

consideration. Additionally, the bombardment does not cause any visible changes of the redistribution of the electronic states within the valence-band region of the studied single crystals. The present XPS results reveal low hygroscopicity of the  $(\text{Ga}_{55}\text{In}_{45})_2\text{S}_{300}$  and  $(\text{Ga}_{54.59}\text{In}_{44.66}\text{Er}_{0.75})_2\text{S}_{300}$  single crystal surfaces. This property is expected to be very important for handling these materials in optoelectronic devices operating at ambient conditions. When going from  $(\text{Ga}_{55}\text{In}_{45})_2\text{S}_{300}$  to  $(\text{Ga}_{54.59}\text{In}_{44.66}\text{Er}_{0.75})_2\text{S}_{300}$ , we have not detected changes of shapes of the XPS core-level and valence-band spectra and shifts of the binding energy position of constituent element core levels. This means that the insertion of  $\text{Er}^{3+}$  ions into the  $(\text{Ga}_{55}\text{In}_{45})_2\text{S}_{300}$  lattice resulting in the formation of the  $(\text{Ga}_{54.59}\text{In}_{44.66}\text{Er}_{0.75})_2\text{S}_{300}$  sample does not change significantly the peculiarities of the chemical bonding of the parent compound.

The X-ray emission Ga  $K\beta_2$  and S  $K\beta_{1,3}$  bands giving information on the energy distribution of the Ga  $4p$  and S  $3p$  states, respectively, have been measured for the  $(\text{Ga}_{55}\text{In}_{45})_2\text{S}_{300}$  single crystal and compared on a common energy scale with its XPS valence-band spectrum. This comparison reveals that the Ga  $4p$  states contribute mainly in the central portion of the valence band of  $(\text{Ga}_{55}\text{In}_{45})_2\text{S}_{300}$ , while principal contributions of the S  $3p$  states are detected at the top of the band, with their contributions in other portions of the valence band of the compound under consideration. Additionally, we have also detected a strong photoluminescence of the  $(\text{Ga}_{54.59}\text{In}_{44.66}\text{Er}_{0.75})_2\text{S}_{300}$  single crystal with a maximum at 810 nm for the excitation wavelength of 532 nm at 300 K. These results coupled with those reported in Ref. [14] allow for concluding that the existence of the two intensive emission bands in the near infrared spectral range is characteristic of the  $(\text{Ga}_{54.59}\text{In}_{44.66}\text{Er}_{0.75})_2\text{S}_{300}$  single crystal. Therefore, the  $(\text{Ga}_{54.59}\text{In}_{44.66}\text{Er}_{0.75})_2\text{S}_{300}$  single crystal is a very promising material for its application in optoelectronic technologies, in particular luminophores, wide-band optical filters, light-emitting diodes, optical amplifiers, etc.

**Acknowledgments** This work was partially supported by the Project of Ministry of Education and Science of Ukraine (No. 0115U 002348).

## References

1. J. Ye, T. Hanada, Y. Nakamura, O. Nittono, Phys. Rev. B **62**, 16554 (2000)
2. C. Sanz, C. Guillen, M.T. Gutierrez, J. Phys. D Appl. Phys. **41**, 235103 (2008)
3. S.P. Hong, H.K. Park, H.J. Oh, J. Mater. Chem. **22**, 18939 (2012)
4. I.A. Ivashchenko, I.V. Danyliuk, I.D. Olekseyuk, V.V. Halyan, J. Solid State Chem. **210**, 102 (2014)
5. V. Kramer, R. Nitsche, J. Cryst. Growth **7**, 285 (1970)
6. R. Nitsche, J. Cryst. Growth **9**, 238 (1971)
7. M. Schulte Kellinghaus, V. Kramer, Z. Naturforsch. B **37**, 390 (1982)
8. G.G. Guseinov, I.R. Amiraslanov, A.S. Kuliev, K.S. Mamedov, Izv. Akad. Nauk SSSR: Neorg. Mater. **23**, 854 (1987)
9. G.G. Guseinov, I.R. Amiraslanov, A.S. Kuliev, Kristallografiya **32**, 140 (1987)
10. G.G. Guseinov, M.G. Kazimov, A.S. Zyliev, Dokl. Akad. Nauk AzSSR **44**, 26 (1988)
11. I.R. Amiraslanov, F.Y. Asadov, B.A. Maksimov, V.N. Molchanov, A.A. Musaev, N.G. Furmanova, Kristallografiya **35**, 332 (1990)
12. I.R. Amiraslanov, Y.G. Asadov, B.B. Valiev, A.A. Musaev, G.G. Guseinov, Kristallografiya **35**, 1298 (1990)
13. G.G. Guseinov, S.M. Eyvazova, V.O. Aliev, V.A. Gasumov, Chem. Chem. Technol. **4**, 62 (2004)
14. I.A. Ivashchenko, I.V. Danyliuk, I.D. Olekseyuk, V.Z. Pankevych, V.V. Halyan, J. Solid State Chem. **227**, 255 (2015)
15. A.H. Reshak, S. Auluck, I.V. Kityk, A. Perona, B. Claudet, J. Phys.: Condens. Matter **20**, 325213 (2008)
16. A.A. Lavrentyev, B.V. Gabrelian, I.Y. Nikiforov, O.V. Parasyuk, O.Y. Khyzhun, J. Alloys Compd. **481**, 28 (2009)
17. A.A. Lavrentyev, B.V. Gabrelian, B.B. Kulagin, I.Ya. Nikiforov, O.Y. Khyzhun, Bull. Russ. Acad. Sci. Phys. **73**, 1140 (2009)
18. A.H. Reshak, S.A. Khan, Mater. Res. Bull. **48**, 4555 (2013)
19. V.L. Bekenev, V.V. Bozhko, O.V. Parasyuk, G.E. Davydyuk, L.V. Bulatetska, A.O. Fedorchuk, I.V. Kityk, O.Y. Khyzhun, J. Electron Spectrosc. Relat. Phenom. **185**, 559 (2012)
20. S.-H. Ma, Z.-Y. Jiao, X.-Z. Zhang, J. Mater. Sci. **47**, 3849 (2012)
21. T. Babuka, I.V. Kityk, O.V. Parasyuk, G. Myronchuk, O.Y. Khyzhun, A.O. Fedorchuk, M. Malowska-Janusik, J. Alloys Compd. **633**, 415 (2015)
22. J.F. Moulder, W.E. Stickle, P.E. Sobol, K.E. Bomben, in *Handbook of X-ray Photoelectron Spectroscopy*, ed. by J. Chastian (Perkin-Elmer, Eden Prairie, 1992)
23. A.Y. Tarasova, L.I. Isaenko, V.G. Kesler, V.M. Pashkov, A.P. Yelisseyev, N.M. Denysyuk, O.Y. Khyzhun, J. Phys. Chem. Solids **73**, 674 (2012)
24. G.L. Myronchuk, G.E. Davydyuk, O.V. Parasyuk, O.Y. Khyzhun, R.A. Andrievski, A.O. Fedorchuk, S.P. Danylchuk, L.V. Piskach, M.Y. Mozolyuk, J. Mater. Sci.: Mater. Electron. **24**, 3555 (2013)
25. O.Y. Khyzhun, Y.V. Zaulychny, E.A. Zhurakovsky, J. Alloys Compd. **244**, 107 (1996)
26. O.Y. Khyzhun, V.L. Bekenev, Y.M. Solonin, J. Alloys Compd. **459**, 22 (2008)
27. E.Z. Kurmaev, V.M. Cherkashenko, L.D. Finkelstein, *X-ray Spectra of Solids* (Nauka, Moscow, 1988)
28. E.A. Zhurakovsky, V.F. Nemchenko, *Kinetic Properties and Electronic Structure of Interstitial Phases* (Naukova Dumka, Kyiv, 1989)
29. A. Meisel, G. Leonhardt, R. Szargan, *X-ray Spectra and Chemical Binding* (Springer, Berlin/Heidelberg, 1989)
30. M.L. Frej, E. Valdez, C.B. de Araújo, Y. Ledemi, Y. Messaddeq, J. Appl. Phys. **108**, 093514 (2010)
31. V.V. Halyan, V.V. Strelchuk, V.O. Yukhymchuk, A.H. Kevshyn, G.Ye. Davydyuk, M.V. Shevchuk, S.V. Voronyuk, Physica B **411**, 35 (2013)
32. V.V. Halyan, A.H. Kevshyn, Yu.M. Kogut, G.Ye. Davydyuk, M.V. Shevchuk, V. Kazukauskas, A. Ziminskij, Phys. Status Solidi C **6**, 2810 (2009)